

# Modification 1T-MoS<sub>2</sub> with surface ions towards electrocatalytic hydrogen evolution reaction

Lulu Chen<sup>1, a</sup>, Yichao Huang<sup>1, b,\*</sup>, Limin Wang<sup>1</sup>, Sixuan Huang<sup>1</sup>,  
Zhuangjun Fan<sup>1, c,\*</sup>

<sup>1</sup>State Key Laboratory of Heavy Oil Processing, School of Materials Science and Engineering, China University of Petroleum, Qingdao, Shandong, 266580, China;

<sup>a</sup> 17860776270@139.com, <sup>b,\*</sup> yichaoh@upc.edu.cn, <sup>c,\*</sup> fanzhj666@163.com.

**Abstract.** Molybdenum disulfide (MoS<sub>2</sub>) is considered as a thriving and cost-efficient electrocatalyst for hydrogen evolution reaction (HER). Unfortunately, the semiconductor phase of 2H-MoS<sub>2</sub> itself has a conservative electronic intrinsic transport rate and the restricted active sites to edge regions, leading to unsatisfactory electrocatalytic performance of HER. Here, we have fabricated highly conductive metal phase 1T-MoS<sub>2</sub> nanosheets by a hydrothermal method and introduced a series of transition metal ions on their surfaces by an in-situ reduction strategy to achieve MoS<sub>2</sub> surface modification. It was found that the metals Ni and Co not only enhanced the intrinsic conductivity of 1T-MoS<sub>2</sub>, but also significantly increased the number of active sites in the catalyst, which resulted in the catalyst exhibiting excellent HER activity. Ni@1T-MoS<sub>2</sub> exhibits fast reaction kinetics (86 mV • dec<sup>-1</sup>), good mechanical stability (~28 h) and low energy consumption in 1.0 M KOH medium, as well as an over-potential of only 187 mV at 50 mA • cm<sup>-2</sup>.

**Keywords:** Hydrogen evolution reaction, Electrocatalysts, 1T-phase MoS<sub>2</sub>.

## 1. Introduction

Hydrogen energy is a principle renewable and clean energy for mankind in the future, its development needs to answer the difficulty of sustainable and clean production of hydrogen energy [1]. Hydrogen production from renewable energy based on electrolytic water is a hopeful way to realize sustainable and hygienic production of hydrogen energy, whereas the cost of this technology is still high [1, 2]. In this regard, the exploitation of cheap and efficient base metal HER electrocatalysts to improve the efficiency and lessen hydrogen production cost has become a current international frontier research issue [2, 3]. In recent years, MoS<sub>2</sub> has been considered as an encouraging base metal HER electrocatalyst, while its performance in electrocatalytic HER is still unsatisfactory [4, 5].

There is a problem that the distribution of active sites is only towards the edges, rendering the electrocatalytic HER performance of MoS<sub>2</sub> less than optimal. [6]. Besides the intrinsic reactivity of the catalytic area and the concentration of catalytically active sites, the electrocatalytic behavior of molybdenum disulfide is also limited by its poor electronic transport properties [7, 8]. As a comparison, the metallic 1T-MoS<sub>2</sub> (Mo-S octahedral coordination mode) has a better electron transport ability and higher electrocatalytic activity than the 2H-MoS<sub>2</sub> (Mo-S trigonal coordination mode) [9, 10]. However, the sub-stable 1T-MoS<sub>2</sub> is inclined to convert into stable 2H-MoS<sub>2</sub> during the reaction process, leading to a decrease in electrocatalytic hydrogen precipitation performance [9]. Accordingly, various strategies such as conductive substrate loading [11], defect engineering [12, 13] and chemical doping [14, 15] have been devoted to the development of electrocatalytic HER property of MoS<sub>2</sub>, but still suffer unstable interfacial electron transport, lack of precise structural design, and ambiguous catalytic sites [16 - 18]. In particular, the properties of 1T-MoS<sub>2</sub> can be greatly modified by different atoms/ions doping, as previously reported by our group, in which the atomic-scale design and synthesis of diatomic Ni/O co-doped NiO@1T-MoS<sub>2</sub>/CFP greatly improved the catalytic properties of 1T-MoS<sub>2</sub>. [14] Therefore, to systematically investigate the interaction of transition metal cation doping/modification towards performance of 1T-MoS<sub>2</sub> is of vital relevance for the optimal design of the catalysts.

In this work, the influence of different ionic modifications on the HER properties of 1T-MoS<sub>2</sub> is explored through a minimalist experimental model. The investigation revealed by introducing different transitional metallic ions onto surface of 1T-MoS<sub>2</sub> can significantly affect the HER activity, and the influences of transition metal ions on the properties of 1T-MoS<sub>2</sub> were as follows: Ni@1T-MoS<sub>2</sub> > Co@1T-MoS<sub>2</sub> > 1T-MoS<sub>2</sub> > Cu@1T-MoS<sub>2</sub> > Mn@1T-MoS<sub>2</sub> > Fe@1T-MoS<sub>2</sub>. In particular, Ni@1T-MoS<sub>2</sub> has the advantages of low overpotential ( $\eta_{50}$ =187 mV) and stable performance (almost 28 hours). It is speculated that this may be due to the fact that the introduction of metallic nickel ions will optimally modify 1T-MoS<sub>2</sub>. With the modification of nickel ions, the conductivity of 1T-MoS<sub>2</sub> was significantly enhanced and the number of active sites will be increased, while at the same time, the electron density on the 1T-MoS<sub>2</sub> surface will be regulated. On this basis, we hypothesized that suitable metal ion modifications could promote the water molecule dissociation ability of the M@1T-MoS<sub>2</sub> catalyst under alkaline conditions and provide sufficient H protons for the HER reaction, thus accelerating the sluggish HER reaction process.

## 2. Experimental Methods

### 2.1 Experimental Section

#### 2.1.1 Synthesis of 1T-MoS<sub>2</sub>

The (NH<sub>4</sub>)<sub>6</sub>Mo<sub>7</sub>O<sub>24</sub>·4H<sub>2</sub>O (0.12 mmol) and thioacetamide (TAA, 2 mmol) were mixed in 30 mL H<sub>2</sub>O, transferred into a 50 mL Teflon autoclave with a 2\*4 cm<sup>2</sup> sheet of hydrophilic carbon fiber paper, and maintained at 180°C for 24 h. Following the reaction, the CFP was taken out and cleaned twice with and purified water, respectively, and then dried in a vacuum oven for 12 hours to get the 1T-MoS<sub>2</sub> catalyst.

#### 2.1.2 Synthesis of M@1T-MoS<sub>2</sub>

A piece of 1\*2 cm<sup>2</sup> was immersed in 0.1 M metal salt solution {Ni(NO<sub>3</sub>)<sub>2</sub>·6H<sub>2</sub>O, Fe(NO<sub>3</sub>)<sub>3</sub>·9H<sub>2</sub>O, Co(NO<sub>3</sub>)<sub>2</sub>·6H<sub>2</sub>O, Cu(NO<sub>3</sub>)<sub>2</sub>·3H<sub>2</sub>O, Mn(CH<sub>3</sub>COO)<sub>2</sub>·4H<sub>2</sub>O}, respectively, and removed after 5 min, followed by drying in an oven at 60°C for 2 h. The corresponding samples were labelled as M@1T-MoS<sub>2</sub> (M=Fe, Co, Ni, Cu, Mn).

### 2.2 Characterization and electrochemical measurements.

Scanning electron microscopy (SEM) and energy dispersive X-ray spectroscopy (EDX) were used to supply morphological and dimensional characterization of the nanomaterials. A HORIBA JY HR800 confocal Raman microscope and an argon ion laser with a wavelength of 532 nm were used to record Raman spectra. Powder X-ray diffraction (XRD) characterization was carried out on an X-ray refractometer using Cu-K $\alpha$  radiation ( $\lambda = 1.5418 \text{ \AA}$ ) at a controlled scanning rate within ten degrees per minute. Electrochemical performance parameters in a 1.0 M KOH electrolyte were evaluated using a CHI760E electrochemical workstation.

### 3. Results and discussions

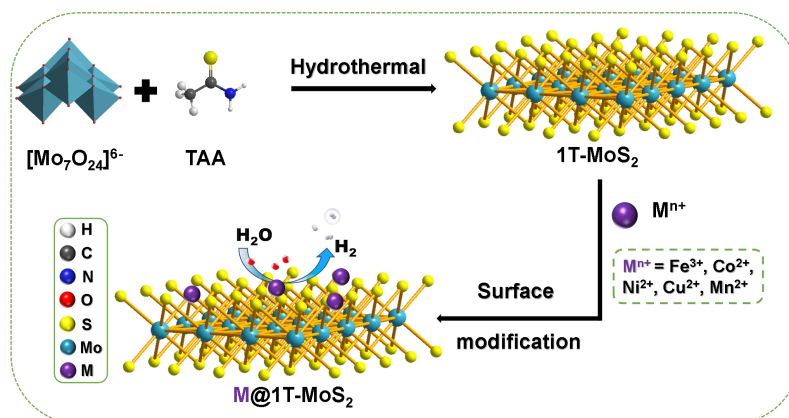


Fig. 1. Schematic depicting of M@1T-MoS<sub>2</sub> electrocatalyst fabrication.

As presented in Fig. 1, 1T-MoS<sub>2</sub> grown in-situ on CFP with one-step hydrothermal method, followed by a simple impregnation method to anchor the metal atoms on the MoS<sub>2</sub> surface under the adsorption of negatively charged and reducing sulfur atoms. It can be observed by scanning electron microscopy (SEM) in Fig. 2 a-e that the surface of the pristine carbon fiber is smooth, and a layer of MoS<sub>2</sub> with irregularly folded nanosheet morphology has been uniformly grown on the surface of the carbon fiber after the hydrothermal reaction, and no obvious agglomeration has been found. The corresponding EDS elemental analysis plots (Fig. 2f-g) verify the homogeneous coexistence of Mo and S elements in the MoS<sub>2</sub> nanosheets. Meanwhile, and the N<sub>2</sub> adsorption-desorption isotherm showed that our synthesized 1T-MoS<sub>2</sub> powder has a large specific surface area (120.46 m<sup>2</sup>·g<sup>-1</sup>), which can provide an adequate reaction space for the HER reaction.

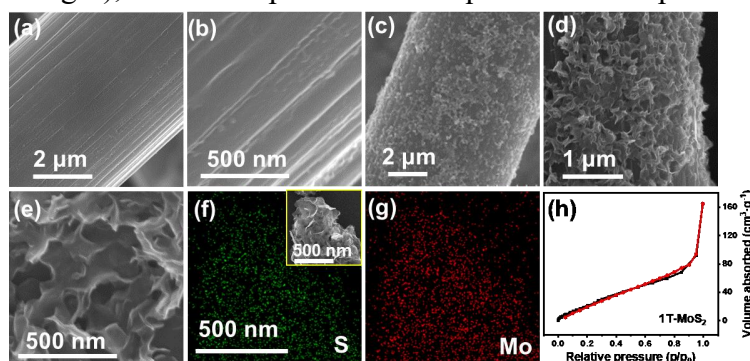


Fig. 2. SEM images of (a-b) CFP and (c-e) 1T-MoS<sub>2</sub>, (f-g) the EDS elemental mapping of Mo, S elements in 1T-MoS<sub>2</sub> electrocatalysts, (h) N<sub>2</sub> adsorption-desorption isotherm of 1T-MoS<sub>2</sub>.

The crystalline phase components of 1T-MoS<sub>2</sub> was further investigated and determined by XRD. As displayed in Fig.3(a), the diffraction peaks of 1T-MoS<sub>2</sub> coincided with the MoS<sub>2</sub> crystals in the standard card (PDF#75-1539), indicating that main phase of catalyst is the target product MoS<sub>2</sub>. Raman spectrum showed that the diffraction peaks of 1T-MoS<sub>2</sub> mainly appeared between 100 and 350 cm<sup>-1</sup>(147,214,236,283, and 335 cm<sup>-1</sup>), which were consistent with the peaks of E12g and A1g of 1T-MoS<sub>2</sub>, and no obvious 2H-MoS<sub>2</sub> diffraction peaks were found [14]. The above characterization results indicate that our synthesized MoS<sub>2</sub> mainly consists of the highly conductive metal phase 1T-MoS<sub>2</sub>, eliminating the problem of poor inherent conductivity faced by 2H-MoS<sub>2</sub> in electrocatalytic reactions, with the advantage of enhancing the fast electron transport in HER and accelerating the HER reaction process.

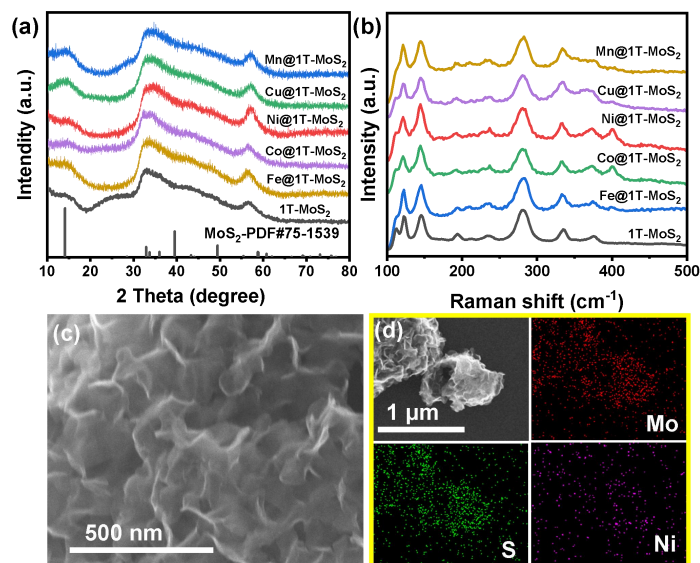


Fig. 3. (a) XRD and (b) Raman of 1T-MoS<sub>2</sub> and M@1T-MoS<sub>2</sub>, (c) SEM of Ni@1T-MoS<sub>2</sub>, (d) EDS spectra of Ni@1T-MoS<sub>2</sub>.

We further investigated the composition and morphology of M@1T-MoS<sub>2</sub> modified with different transition metal ions. The XRD peak positions and geometries of M@1T-MoS<sub>2</sub> exhibited no significant changes after the introduction of different transition metals (see in Fig. 3a), indicating that no new physical phases appeared. The Raman spectra (Fig. 3b) exhibits the M@1T-MoS<sub>2</sub> modified with different metal atoms, while their phases still remain metallic, suggesting that the doping of surface atoms does not cause any undesirable phase transition of 1T-MoS<sub>2</sub>, and also confirming that our prepared 1T-MoS<sub>2</sub> has a good stability. The SEM of Ni@1T-MoS<sub>2</sub> (shown in Fig. 3c) results show that the introduction of Ni atoms still maintains the original wrinkled layer structure of 1T-MoS<sub>2</sub>, which does not affect the morphology of 1T-MoS<sub>2</sub>, while the EDS elemental distribution maps in Fig. 3d further illustrates that Ni, Mo and S atoms are homogeneously coexisting in Ni@1T-MoS<sub>2</sub>, implying that Ni atoms are successfully introduced into 1T-MoS<sub>2</sub>.

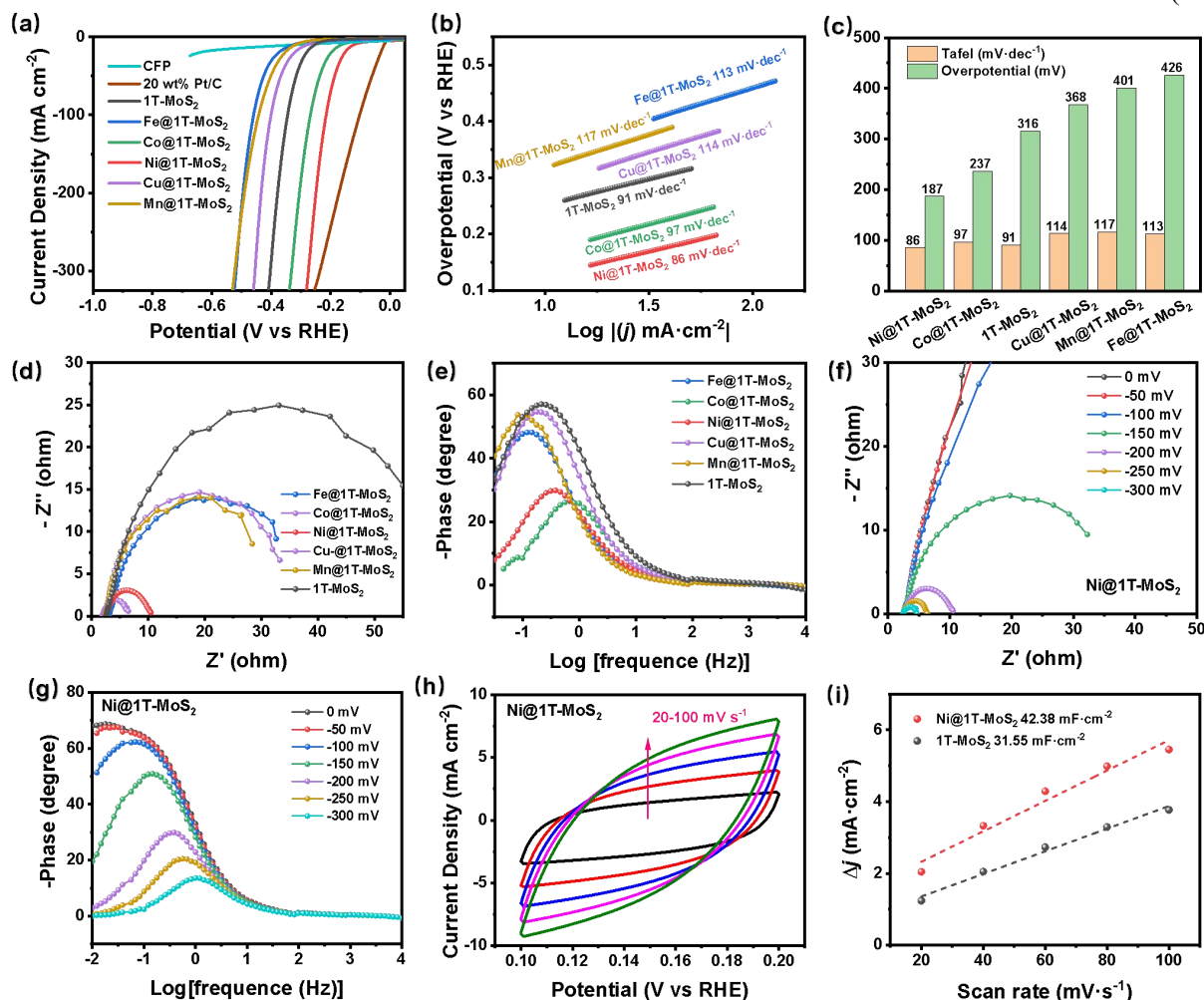


Fig. 4. HER catalytic performances in alkaline media. (a) LSV curves; (b) Tafel plots; (c) Histogram of overpotentials ( $j = 50 \text{ mA}\cdot\text{cm}^{-2}$ ) and Tafel values; (d) Nyquist and (e) Bode Plots of samples; (f) Nyquist and (g) Bode plots of Ni@1T-MoS<sub>2</sub>; (h)  $C_{dl}$  value; (i) Stability evaluation.

In order to evaluate the effect of modification of 1T-MoS<sub>2</sub> with different metal ions on HER properties, the electrocatalytic activity of M@1T-MoS<sub>2</sub> in alkaline electrolyte was employed. Ni@1T-MoS<sub>2</sub> requires only a small overpotential (86 mV) to reach a current density of 50 mA·cm<sup>-2</sup> (As shown in Fig. 2a). It is slightly inferior to commercial Pt/C catalysts, but significantly better than other M@1T-MoS<sub>2</sub> as well as 1T-MoS<sub>2</sub> samples. By calculating the Tafel slope, the reaction kinetics of the above-mentioned catalysts can be evaluated (Fig.4b). The smaller Tafel slope (86 mV·dec<sup>-1</sup>) for Ni@1T-MoS<sub>2</sub> compared to the other samples indicates a faster electrochemical reaction kinetics, suggesting that the Ni@1T-MoS<sub>2</sub> electrocatalysts are reacting via the Volmer-Heyrovsky (V-H) mechanism [19]. In order to more visually represent the difference in the performance of each catalyst material, a histogram of overpotential versus Tafel value is given in Fig. 4c, indicating that Ni@1T-MoS<sub>2</sub> is the most preferred efficient HER catalyst [20].

With the purpose of understanding in depth the effect of transition metal atom modification on the conductivity and reaction kinetics on the 1T-MoS<sub>2</sub> surface, we have performed electrochemical impedance tests on M@1T-MoS<sub>2</sub> at specific potentials. The minimum semicycle diameter shown by Ni@1T-MoS<sub>2</sub> and Co@1T-MoS<sub>2</sub> in Nyquist diagram in Fig. 4d indicates that the conductivity of 1T-MoS<sub>2</sub> is remarkably increased, while the reduced phase angle of the Bode plot in the high-frequency region (Heyrovsky-step) of Fig. 4e suggests a faster reaction during the HER reaction of Ni@1T-MoS<sub>2</sub> versus Co@1T-MoS<sub>2</sub> with faster reaction kinetics [21]. The Nyquist versus Bode plots of Ni@1T-MoS<sub>2</sub> at different potentials indicate the electrocatalytic reaction as a V-H mechanism. Heyrovsky step was improved due to much lower charge transfer resistance and

very high hydrolysis dissociation efficiency in Ni@1T-MoS<sub>2</sub> catalysts, resulting in higher HER activity than other catalysts [22]. The corresponding effective electrochemically active surface area (ECSA) was estimated from the cyclic voltammetry curves at different scanning rates (Figure 4h) to calculate the double-layer capacitance (Cdl). In Fig. 4e, the Cdl of Ni@1T-MoS<sub>2</sub> is 42.38 mF cm<sup>-2</sup>, superior to that of 1T-MoS<sub>2</sub> (31.55 mF cm<sup>-2</sup>), implying that the adsorption of appropriate amount of Ni atoms on the surface of 1T-MoS<sub>2</sub> can effectively increase the electrochemical active area to expose more active sites. In accordance with the above results, it can be concluded that the effects of various transition metal ions on the behaviour of 1T-MoS<sub>2</sub> are as follows: Ni@1T-MoS<sub>2</sub> > Co@1T-MoS<sub>2</sub> > 1T-MoS<sub>2</sub> > Cu@1T-MoS<sub>2</sub> > Mn@1T-MoS<sub>2</sub> > Fe@1T-MoS<sub>2</sub>.

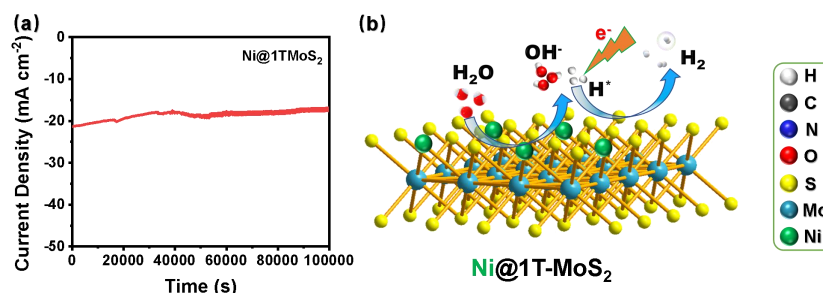


Fig. 5 (a) i-t curve of Ni@1T-MoS<sub>2</sub>, (b) Schematic diagram of the HER reaction on the Ni@1T-MoS<sub>2</sub> surface.

Ultimately, we assessed the robustness of the catalysts presented in Fig. 5a, the current density of Ni@1T-MoS<sub>2</sub> showed barely visible decline after testing at specific potentials for up to 30 h using the chronopotential method, indicating that the catalyst has good stability. Based on the above experimental results, we speculate that the appropriate introduction of transition metal atoms on the surface of 1T-MoS<sub>2</sub> can effectively improve the surface properties of the catalytic material and accelerate the HER process (as shown in Fig. 5b). The introduction of appropriate metal ions can effectively improve the hydrolysis dissociation ability during the HER reaction process, as well as optimize the adsorption energy of intermediates to enhance the overall HER performance [14].

## 4. Summary

In conclusion, the introduction of different transition metal atoms doped on 1T-MoS<sub>2</sub> nanosheets increased the electrocatalytic active sites, providing an opportunity to significantly modulate the electronic structure and accelerate the slow kinetics of HER. Among the various catalysts tested in this study, Ni@1T-MoS<sub>2</sub> showed the most prominent HER activity with a minimum overpotential, a small Tafel slope (86 mV dec<sup>-1</sup>), and excellent mechanical stability in basic media (approximately 28 hours). The experimental results show that the introduction of suitable transition metal atoms on ultrathin 1T-MoS<sub>2</sub> nanosheets can effectively promote the hydrogen generation process. It is speculated that this excellent performance may be attributed to the introduction of metallic Ni and Co ions, which not only enhance the electrical conductivity of 1T-MoS<sub>2</sub>, but also modify the electron density on the MoS<sub>2</sub> surface, facilitate the splitting of aqueous molecules under basic environment, as well as supply sufficient H protons for the HER reaction, and thus accelerate the sluggish kinetics in HER process. However, the electron effect of surface atomic modification and its influence on the adsorption free energy of intermediates involved in HER process still need to be further studied, as we will pursue further studies and explorations in our further work. Undeniably, the modification of different transition metal atoms is a feasible option to enrich the intrinsic electrocatalytic activity of 1T-MoS<sub>2</sub>.

## References

- [1] Chatenet M, Pollet B. G, Dekel D. R, et al. Water electrolysis: from textbook knowledge to the latest scientific strategies and industrial developments. *Chemical Society Reviews*, 2022, 51 (11): 4583-4762.

- [2] Wang J, Liao T, Wei Z, et al. Heteroatom-Doping of Non-Noble Metal-Based Catalysts for Electrocatalytic Hydrogen Evolution: An Electronic Structure Tuning Strategy. *Small Methods*, 2021, 5 (4), e2000988.
- [3] Yu Z. Y, Duan Y, Feng, X. Y, et al. Clean and Affordable Hydrogen Fuel from Alkaline Water Splitting: Past, Recent Progress, and Future Prospects. *Advanced Materials*, 2021, 33 (31): e2007100.
- [4] Wu X, Zhang H, Zhang J, et al. Recent Advances on Transition Metal Dichalcogenides for Electrochemical Energy Conversion. *Advanced Materials*, 2021, 33 (38): e2008376.
- [5] Wang, M.; Zhang, L.; He, Y. J.; Zhu, H. W., Recent advances in transition-metal-sulfide-based bifunctional electrocatalysts for overall water splitting. *Journal of Materials Chemistry A*, 2021, 9 (9): 5320-5363.
- [6] Xia H, Shi Z, Gong C, et al. Recent strategies for activating the basal planes of transition metal dichalcogenides towards hydrogen production. *Journal of Materials Chemistry A*, 2022, 10(37): 19067-19089.
- [7] Zhu D, Liu J, Zhao Y, et al. Engineering 2D Metal-Organic Framework/MoS<sub>2</sub> Interface for Enhanced Alkaline Hydrogen Evolution. *Small*, 2019, 15 (14): e1805511.
- [8] Wei X, Lin C.C, Wu C, et al. Three-dimensional hierarchically porous MoS<sub>2</sub> foam as high-rate and stable lithium-ion battery anode. *Nature Communications*, 2022, 13 (1): 6006.
- [9] Guo X, Song E, Zhao W, et al. Charge self-regulation in 1T'-MoS<sub>2</sub> structure with rich S vacancies for enhanced hydrogen evolution activity. *Nature Communications*, 2022, 13 (1): 5954.
- [10] Lin Y.C, Dumcenco D.O, Huang Y.S, et al. Atomic mechanism of the semiconducting-to-metallic phase transition in single-layered MoS<sub>2</sub>. *Nature Nanotechnology*, 2014, 9 (5): 391-6.
- [11] Liang Z, Sun B, Xu X, et al. Metallic 1T-phase MoS<sub>2</sub> quantum dots/g-C<sub>3</sub>N<sub>4</sub> heterojunctions for enhanced photocatalytic hydrogen evolution. *Nanoscale*, 2019, 11 (25): 12266-12274.
- [12] Tsai C, Li H, Park S, et al. Electrochemical generation of sulfur vacancies in the basal plane of MoS<sub>2</sub> for hydrogen evolution. *Nature Communications*, 2017, 8, 15113.
- [13] Li H, Du M, Mleczko M.J, et al. Kinetic Study of Hydrogen Evolution Reaction over Strained MoS<sub>2</sub> with Sulfur Vacancies Using Scanning Electrochemical Microscopy. *Journal of the American Chemical Society*, 2016, 138 (15): 5123-9.
- [14] Huang Y, Sun Y, Zheng X, et al. Atomically engineering activation sites onto metallic 1T-MoS<sub>2</sub> catalysts for enhanced electrochemical hydrogen evolution. *Nature Communications*, 2019, 10 (1): 982.
- [15] Qi K, Cui X, Gu L, et al. Single-atom cobalt array bound to distorted 1T MoS<sub>2</sub> with ensemble effect for hydrogen evolution catalysis. *Nature Communications*, 2019, 10 (1): 5231.
- [16] Li J, Listwan A, Liang J, et al. High proportion of 1T phase MoS<sub>2</sub> prepared by a simple solvothermal method for high-efficiency electrocatalytic hydrogen evolution. *Chemical Engineering Journal*, 2021, 422, 130100.
- [17] Zhai P, Zhang Y, Wu Y, et al. Engineering active sites on hierarchical transition bimetal oxides/sulfides heterostructure array enabling robust overall water splitting. *Nature Communications*, 2020, 11 (1): 5462.
- [18] Sun B, Liang Z, Qian Y, et al. Sulfur Vacancy-Rich O-Doped 1T-MoS<sub>2</sub> Nanosheets for Exceptional Photocatalytic Nitrogen Fixation over CdS. *ACS Applied Materials & Interfaces*, 2020, 12 (6): 7257-7269.
- [19] Chen L, Jang H, Kim M.G, et al. Fe<sub>x</sub>Ni<sub>y</sub>/CeO<sub>2</sub> loaded on N-doped nanocarbon as an advanced bifunctional electrocatalyst for the overall water splitting. *Inorganic Chemistry Frontiers*, 2020, 7 (2): 470-476.
- [20] Chen L, Jang H, Kim M.G, et al. Fe, Al-co-doped NiSe<sub>2</sub> nanoparticles on reduced graphene oxide as an efficient bifunctional electrocatalyst for overall water splitting. *Nanoscale*, 2020, 12 (25): 13680-13687.
- [21] Zhang Y, Arpino K.E, Yang Q, et al. Observation of a robust and active catalyst for hydrogen evolution under high current densities. *Nature Communications*, 2022, 13 (1): 7784.
- [22] Chen W, Wu B, Wang Y, et al. Deciphering the alternating synergy between interlayer Pt single-atom and NiFe layered double hydroxide for overall water splitting. *Energy & Environmental Science*, 2021, 14 (12): 6428-6440.